A Comprehensive Performance Analysis of Direct Detection Receivers in WDMA Systems

M. Moulavi-Kakhki[1] D. Rejaly[2]

[1] Associate Professor, Faculty of Electrical Engineering, Ferdowsi University of Mashhad, Mashhad, Iran

Email: molavi_kh@yahoo.com

[2] M. Sc., Faculty of Electrical Engineering, Ferdowsi University of Mashhad, Mashhad, Iran

Email: drejaly@um.ac.ir

Abstract:

In this work the performance of a wavelength division multiple access (WDMA) system with direct detection receiver is investigated. For this purpose, the probability of error in a WDMA network with OOK modulation considering crosstalk, ISI, photo detector noise and thermal noise is calculated and the effect of each on system performance is investigated. The system performance in presence of PIN and APD Photo detectors are compared. Besides the accurate calculations of bit error rate, these calculations have also been performed using Gaussian, Chernoff bound and modified Chernoff bound approximations for the decision variable. Results of our calculations of the photo detector noise penalty in presence PIN and APD photo detectors are presented and compared for different number of channels. Also, from the calculations of the receiver sensitivity, an optimum value for the avalanche gain of APD is obtained. The superiority of APD over PIN photo detection is also demonstrated.

Keywords: Wavelength division multiple access (WDMA), Photo detectors, Direct detection receivers

Submission date: March 3, 2005

Acceptance date: July 4, 2008

Corresponding author: M. Moulavi-Khaki

Address of corresponding author: Faculty of Electrical Engineering, Ferdowsi University of Mashhad, Mashhad, Iran

1. Introduction

Wavelength division multiplexing as means of achieving high capacity communication systems has been the subject of interest for many years [1-9]. An M-channel WDMA system consists of a laser diode, a star coupler and an optical filter at the receiver for channel selection. Photo detection is performed by a PIN or an avalanche photo detector (APD).

Due to the modest selectivity of optical filters crosstalk is inevitable in WDMA systems and can impose serious limitations upon their performance. Crosstalk degradation in these systems has been studied by many authors. Kaminow et al. [1] have presented theoretical and experimental results for crosstalk degradation in a WDMA network with FSK modulation. Li and his co-workers [10] have optimized the channel capacity of WDMA systems in presence of laser chirp and crosstalk by a simulation approach. Cimini et al. [11] have shown that the spectral efficiency of WDMA systems with direct detection can be improved by multilevel signaling. Crosstalk degradation in WDMA systems have been reported by Hill and Payne [12], Rosher and Hanwicks [13] and Geckler [14]. In these works the worst case eye – opening for estimating the system performance has been considered. Crosstalk degradations employing Fabry-Perot and Mach-Zehnder filters have also been investigated by Hamdy and Humbelt [15]. In their work, crosstalk signal has been considered as a stochastic process for estimating the system performance. They have used PIN photo diode as a photo detector and assumed that shot noise is negligible with respect to the receiver thermal noise.

In this paper by considering shot noise, the work of Hamdy and Humbelt [15] is completed. Here, we calculate the probability of error in a WDMA system with direct detection and OOK modulation in presence of crosstalk, intersymbol interference (ISI), photo detector noise and post detection thermal noise. It is shown that in this multichannel system the shot noise degrading effect increases with increase in the number of channels. We also show that when APD is used as the photo detector, there is an optimum practical gain for APD that improves the receiver performance.

Error probability for both APD and PIN photo detectors is calculated using two different statistical approaches: i) *accurate method,* in which the non Gaussian part of the decision variable is derived in a rigorous manner. ii) *approximate method,* in which the overall decision variable (sum of Gaussian and non Gaussian parts) is considered as a Gaussian, Chernoff bound, and modified Chernoff bound random variable. Among these, the Chernoff bound proved to be the most accurate approximation for the decision variable.

In section 2 the system model is introduced. In this section the models of transmitter, signal and receiver are presented. The decision variable which is the key parameter for our calculations is introduced and its statistics are derived in sections 3. In section 4 the statistics of the incident optical energy is presented. Computation of the probability of error is presented in section 5. Results and discussion are presented in section 6. Power penalty and receiver sensitivity of the system with different number of channels are also included in this section. Conclusion is presented in section 7.

2. System Model

2.1. Signal Model

The transmitter is assumed to consist of M multiplexed channels as shown in Fig. 1. The channels are equiespaced with spacing $\Delta f = P/M$ where P is the system bandwidth.

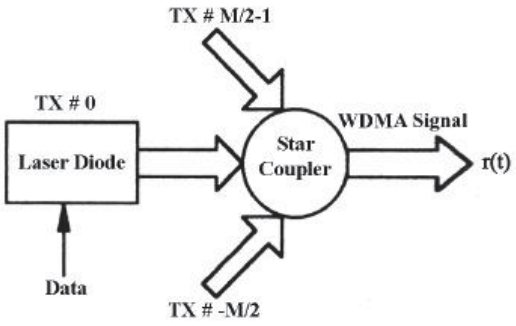

Fig.1: WDMA-OOK network

Channel numbers range from –M/2 to M/2-1. Channel 0 is chosen to be the desired channel and the other M-1 channels are the crosstalk channels.

In this model the channels are assumed to be synchronous with equal bit rates and NRZ pulse shapes.

Let P(t) be the baseband pulse shape in each of the M transmitters. Using the complex envelope notation the multiplexed signal r(t) may be written as:

$$r(t) = \sum_{i=-M/2}^{M/2-1} \sum_{k=-\infty}^{+\infty} d_{ik}\, p(t - kT) e^{j(2\pi\Delta f_i + \varphi_i)} \qquad (1\text{-}1)$$

Where f_i and φ_i are the carrier frequency and phase of channel i respectively and $\Delta f_i = f_i - f_o$. $d_{ik} \in \{0,1\}$ is the transmitted data by channel i in time interval [kT, (k+1)T] in which T is the bit duration. If $p_i(t)$ is defined as :

$$p_i(t) = p(t)e^{j2\pi\Delta f_i t} \qquad (1\text{-}2)$$

The pulse shape P(t) is a non return to zero (NRZ) pulse.

The WDMA signal r(t) can then be written as:

$$r(t) = \sum_{k=-\infty}^{+\infty} d_{ok} p_o(t-kT)e^{j2\pi\varphi_0} + \sum_{\substack{i=-M/2 \\ i\neq 0}}^{M/2-1} \sum_{k=-\infty}^{+\infty} d_{ik} p_i(t-kT)e^{j\varphi_i} \qquad (2)$$

The first term in (2) is the desired signal and the second term is the crosstalk.

2.2. Receiver Model

The direct detection receiver model for OOK modulation is presented in Fig. 2. The receiver consists of an optical filter for channel selection, PIN or APD photo detector and an integrate and dump filter (I&D) which serves as a match filter. The samples of the I&D filter output taken at times t =kT are the decision variables. Each decision variable Z is compared to a decision threshold β in order to estimate the transmitted bit during the corresponding interval.

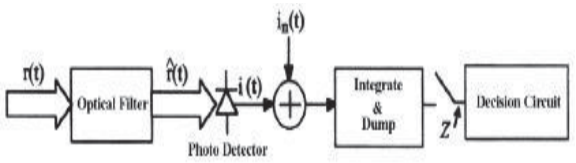

Fig. 2: Direct detection reciever

In this work a Fabry-Perot filter with free spectral range P equal to the system bandwidth is employed as the channel selecting filter. As shown in Fig. 2, i(t) is the output current (photo current) of the photo diode and $i_n(t)$ is the receiver thermal noise which is assumed to be a white zero mean Gaussian process with power spectral density $No/2$ (Amp^2/Hz).

3. Statistics of the Decision Variable

From Fig. 2, the decision variable Z is composed of two components, one is due to the photo current $i(t)$ and the other is due to the thermal noise current $i_n(t)$, i.e. :

$$Z = Z' + N = \frac{1}{e}\int_{\rho}^{\rho+T} i(t)dt + \frac{1}{e}\int_{\rho}^{\rho+T} i_n(t)dt \qquad (3)$$

where Z' and N are photo current and thermal noise components respectively, e is the electron charge and ρ is the offset integration time. The coefficient $1/e$ is for convenience.

The random variable Z conditioned on the photo current i(t) is a Gaussian r.v. with mean Z' and variance $\sigma_N^2 = NoT/2e^2$. Since i(t) and $i_n(t)$ are independent, the moment generating function (MGF) of Z, defined as $E\{e^{sZ}\}$, can be written as:

$$\Phi_z(s) = \Phi_{z'}(s)\Phi_N(s) \qquad (4)$$

in which $\Phi_{z'}(s)$ and $\Phi_N(s)$ are the MGFs of Z' and N respectively and $\Phi_N(s) = \exp(1/2\sigma_N^2 s^2)$. The random variable Z is the key parameters in our analysis, hence, its MGF is require. From eq.(4) , since $\Phi_N(z)$ is known, we only require the MGF of the random variable Z'. A detailed analysis of the statistical properties of Z' and its MGF are presented in the appendix.

For ideal PIN photo detector and ideal I&D filter the moment generating function (MGF) of Z' becomes [16]:

$$\Phi_{Z'}(s) = \Phi_X(e^s - 1) \qquad (5)$$

The right hand side of (5) is the MGF of X when s is substituted by $e^s - 1$ and the random variable X is proportional to the incident optical energy in time interval $[\rho, \rho+T]$ given by:

$$X = \int_{\rho}^{\rho+T} \lambda(t)dt \qquad (6)$$

where $\lambda(t)$ is the rate of photoelercton creation given by:

$$\lambda(t) = \frac{\eta}{h\nu}|\hat{r}(t)|^2 + \lambda_0 \qquad (7)$$

η and $h\nu$ are the quantum efficiency of the photo diode and the photon energy respectively, $\hat{r}(t)$ is the output of the optical filter corresponding to the desired channel and λ_o is the emission rate due to the dark current.

When APD is employed as a photo detector, the conditional MGF becomes [17] :

$$\Phi_{Z'}(s) = \Phi_X(\Phi_G(s) - 1) \tag{8}$$

where $\Phi_G(s)$ is the moment generating function of the random gain G. Implicit and explicit expressions for $\phi_G(s)$ have been presented by different authors [17-19]. In this work the following explicit expression presented by Personick [18] is employed:

$$\Phi_G(s) = \frac{F}{(F-1)^2}\left\{1 - \left[1 - 2s(F-1)\overline{G}\right]^{1/2}\right\} - \frac{1}{F-1}s\overline{G} + 1 \tag{9}$$

where $F = \gamma\overline{G} + \left(2 - \left(1/\overline{G}\right)\right)(1-\gamma)$ is the *excess noise factor* of APD, $\overline{G}$ is the average gain and γ is the ionization rate ratio.

4. Statistics of the Incident Optical Energy

In this section we derive an expression for the MGF of the random variable X given by (6) which depends on the desired and crosstalk channels. For this purpose a model similar to the one presented by Hamdy and Humblet [15] has been employed.

If $h_o(t)$ is the impulse response of the channel selecting optical filter, the filtered passband pulse shape will be $\hat{P}(t) = p_i(t) * h_o(t)$. Hence, the output $\hat{r}(t)$ of the optical filter becomes:

$$\hat{r}(t) = \sum_{k=-\infty}^{k=+\infty} d_{ok}\hat{p}_o(t - kT)e^{j\varphi_o} + \sum_{\substack{i=-M/2 \\ i\neq 0}}^{M/2-1}\sum_{k=-\infty}^{+\infty} d_{ik}\hat{p}_i(t - kT)e^{j\varphi_i} \tag{10}$$

From (6), (7), and (10), we obtain :

$$X = \frac{\eta}{hv}(S + C + C_n) + \lambda_0 T \tag{11}$$

in which :

$$S = \int_{\rho}^{\rho+T}\left|\sum_{k=-\infty}^{+\infty} d_{ok}\hat{p}(t - kT)\right|^2 dt \tag{12}$$

and:

$$C = \sum_{\substack{i=-M/2 \\ i\neq 0}}^{M/2-1}\int_{\rho}^{\rho+T}\left|\sum_{k=-\infty}^{+\infty} d_{ik}\hat{p}_i(t - kT)\right|^2 dt \tag{13-1}$$

and:

$$C_n = 2\int_{\rho}^{\rho+T} A.B\ \cos(\varphi_0 - \varphi_i)dt \tag{13-2}$$

where, A and B are the magnitudes of the first and the second part in the right hand side of (10) respectively.

S is the signal component that is due to the desired channel and C is the linear crosstalk component. C_n in (13-2) corresponds to the nonlinear crosstalk component due to the square law behavior of the photo detector. In fact C_n arises from the multiplication of the two terms in $\hat{r}(t)$ when $|\hat{r}(t)|$ is squared. The nonlinear crosstalk is negligible and can be minimized by choosing $T.\Delta f = k$, where k is an integer and Δf in the channel spacing[15]. This condition has been satisfied in our calculations. With the assumption that S and C are independent, from (11) the MGF of X is given by :

$$\Phi_X(s) = \Phi_S(\alpha s)\Phi_C(\alpha s)e^{s\lambda_o T} \tag{14}$$

where $\alpha = \eta/hv$. To calculate $\Phi_X(s)$, MGFs of the components S and C are required.

4.1. MGF of the Signal Component S

The signal component S in (12) corresponds to the signal bit energy and ISI . Here, the ISI due to the two adjacent bits is only assumed significant. Hence, when ONE is transmitted there are four possible values for S depending on the two adjacent bits. This is also true when ZERO is transmitted. Therefore, if $\Phi_{s_0}(s)$ and $\Phi_{s_1}(s)$ are the conditional MGFs conditioned on the transmitted ONE and ZERO respectively, we can write :

$$\Phi_{S_o}(s) = \frac{1}{4}\sum_{m=1}^{4}\exp(sS_{om}) \qquad (15)$$

$$\Phi_{S_1}(s) = \frac{1}{4}\sum_{m=1}^{4}\exp(sS_{1m}) \qquad (16)$$

in which, S_{1m} and S_{0m} $(m=1,...,4)$ represent the four possible values of S. For example, m=1 corresponds to 000 or 010 and m=2 corresponds to 100 or 110 where the middle bit is the transmitted bit. Hence :

$$S_{om} = \int_{\rho}^{\rho+T}\left|\sum_{k=-1}^{+1} d_{ok}\hat{p}(t-kT)\right|^2 dt, \quad d_{00}=0 \qquad (17)$$

$$S_{1m} = \int_{\rho}^{\rho+T}\left|\sum_{k=-1}^{+1} d_{ok}\hat{p}(t-kT)\right|^2 dt, \quad d_{00}=1 \qquad (18)$$

4.2. MGF of The Crosstalk Component C

Neglecting ISI in crosstalk channels and assuming infinite integration time, the crosstalk component may be written as:

$$C \approx \sum_{\substack{i=-M/2 \\ i\neq 0}}^{M/2-1} d_{io}\, E_i \qquad (19)$$

where E_i is the interfering energy from channel i and is given by :

$$E_i = \int_{-\infty}^{+\infty}\left|\hat{P}_i(t)\right|^2 dt \qquad (20)$$

For equiprobable bits and independent crosstalk channels, the MGF of C can be written as:

$$\Phi_C(s) = \frac{1}{2}\prod_{\substack{i=-M/2 \\ i\neq 0}}^{M/2-1}[\exp(sE_i)+1] \qquad (21)$$

5. Calculation of the Error Probbabiity

The average probability of error, P_e, is given by:

$$P_e = P_o.\Pr\{Z_o > \beta\} + P_1.\Pr\{Z_1 < \beta\} \qquad (22)$$

Where p_i is the prior probability and z_i is the decision variable corresponding to the transmitting bit $i \in (0,1)$ and β is the decision threshold. Note that since shot noise is signal dependent, the statistics of the decision variables corresponding to ZERO and ONE are different. It is evident from (22) that the key factor in error calculation is the PDF of the decision variable Z . In this work two methods have been employed to calculation of error probability. In the first method which is called *accurate,* first the PDF of Z', the non Gaussian part of the decision variable Z in (3) is derived from its MGF and then the PDF of Z is evaluated. In the second method which is called *approximate*, the PDF of the decision variable Z is approximated by a Gaussian, Chernoff bound, and modified Chernoff bound. Note that in both motheds the thermal noise N is a zero mean Gaussian r.v. with variance $\sigma_N^2 = NoT/2e^2$.

5.1. Accurate Method

From (3), the r.v. Z conditioned on Z' is a Gaussian r.v. with mean Z' and variance σ_N^2. Hence, the conditional average probability of error when

$p_0 = p_1$ is:

$$p_{e/z'} = \frac{1}{2}Q\left[\frac{\beta - z_0'}{\sigma_N}\right] + \frac{1}{2}Q\left[\frac{z_1' - \beta}{\sigma_N}\right] \qquad (23)$$

where $Q(x) = \frac{1}{\sqrt{2\pi}}\exp\left(-x^2/2\right)$ and Z_i' is the non – Gaussian part of Z when the transmitting bit is i. The average probability of error is obtained by averaging $p_{e/z'}$, i.e.:

$$p_e = \frac{1}{2}E_{Z_o'}\left\{Q\left[\frac{\beta - Z_0'}{\sigma_N}\right]\right\} + \frac{1}{2}E_{Z_1'}\left\{Q\left(\frac{Z_1' - \beta}{\sigma_N}\right)\right\} \qquad (24)$$

To evaluate the expectations in (24), the PDF of the r.v. z'_i, $p_{Z_i'}(z_i')$ is required which is calculated from its MGF $\Phi_{z_i'}(j\omega)$ using the inverse discrete Fourier transform :

$$p_{z_i'}(z_i') = \mathrm{IDFT}\left[\Phi_{Z_i'}(-j\omega)\right] \qquad (25)$$

where $\Phi_{z_i'}(-j\omega)$ for PIN and APD are given by (5) and (8) respectively.

5.2. Approximate Method

5.2.1. Gaussian Approximation

If the decision variable Z is approximated by a Gaussian r.v, the optimum threshold β_{GA} and the error probability p_{GA} would be:

$$\beta_{GA} = \frac{m_1 \sigma_o + m_o \sigma_1}{\sigma_o + \sigma_1} \qquad (26)$$

and :

$$p_{GA} = Q\left[\frac{m_1 - m_o}{\sigma_1 + \sigma_o}\right] \qquad (27)$$

m_i is the mean and σ_i^2 is the variance of the decision variable Z_i. These parameters were derived by differentiating the MGF presented in section 3.

5.2.2. Chernoff Bound Approximation

The Chernoff bounds for the random variable Z with MGF $\Phi_z(s)$ are given by [20] :

$$\Pr\{Z > \beta\} \le \Phi_z(s)\exp(-\beta s), \quad s > 0 \qquad (28)$$

$$\Pr\{Z < \beta\} \le \Phi_z(s)\exp(-\beta s), \quad s < 0 \qquad (29)$$

The tightest bounds are obtained by minimizing the bounds with respect to *S*. Substituting (28) and (29) in (22) yields to an upper bound for the error probability, P_{CB}, as:

$$P_{CB} = \frac{1}{2}\Phi_{Z_0}(s_0)e^{-\beta s_o} + \frac{1}{2}\Phi_{z_1}(s_1)e^{-\beta s_1} \quad s_0 > 0, s_1 < 0 \qquad (30)$$

where $\Phi_{z_i}(s)\exp(-\beta s)$ is minimum at $s=s_i$ (i=0,1).

5.2.3. Modified Chernoff Bound (MCB)

An improved Chernoff bound for the r.v. Z exists as follow [21]:

$$\Pr\{Z > \beta\} \le \frac{\Phi_{z'}(s)}{\sqrt{2\pi s\sigma_N}}\exp(-\beta s + \sigma_N^2 s^2/2), \quad s > 0 \ (31)$$

$$\Pr\{Z < \beta\} \le \frac{\Phi_{z'}(s)}{\sqrt{2\pi s\sigma_N}}\exp(-\beta s + \sigma_N^2 s^2/2), \quad s < 0 \ (32)$$

The tightest form of these bounds can be obtained by minimizing the upper bound. However, substituting (31) and (32) in (22) leads to the following equation for the upper bound of the error probability:

$$P_{CB} = \frac{1}{2\sqrt{2\pi\sigma_N}}\sum_{i=0}^{1}\frac{1}{s_i}\Phi_{z_i'}(s_i)\exp\left\{-\beta s_i + \sigma_N^2 s_i^2/2\right\} \ (33)$$

Where s_i's are the minimum points of the upper bounds.

6. Results and Discussions

Results of our calculations of the PDF of z', the non-Gaussian part of the decision variable in (3), for both ZERO and ONE as the transmitting bits in a 40 - channel WDMA system for two different input powers(-45 dBm and –35dBm) are presented in Fig. 3. In these calculations the bit rate is 2 Gb/s and a PIN diode is used as a photo detector. A FP filter with FWHM of 4 GHZ and finess of 100 has been employed as the optical selecting filter. In Fig. 3 the results of our calculations when shot noise is taken into account and when it is neglected are compared. The PDF in each case is broader when shot noise is taken into account. This is due to the increases in randomness of the decision variable as a result of shot noise. Note that since shot noise is signal dependent, its effect on the PDF is different for ZERO and ONE. As can be seen from Fig. 3, for the larger input power (Fig. 3b) the two probability functions (solid and dashed lines) are closer than the corresponding case for the smaller input power (Fig. 3a), in other words, as the input power increases, the impact of shot noise on system performance decreases. This is because the variances of crosstalk and ISI are proportional to the square of the input power while the variance of shot noise is proportional to the input power itself, hence, as the input power increases, shot noise is more influenced by ISI and crosstalk. Similar calculations when an APD is employed as the photo detector have resulted in broader probability functions than the PIN case. This is due to the APD's random gain appended to the randomness of the releasing primary electrons (shot noise).

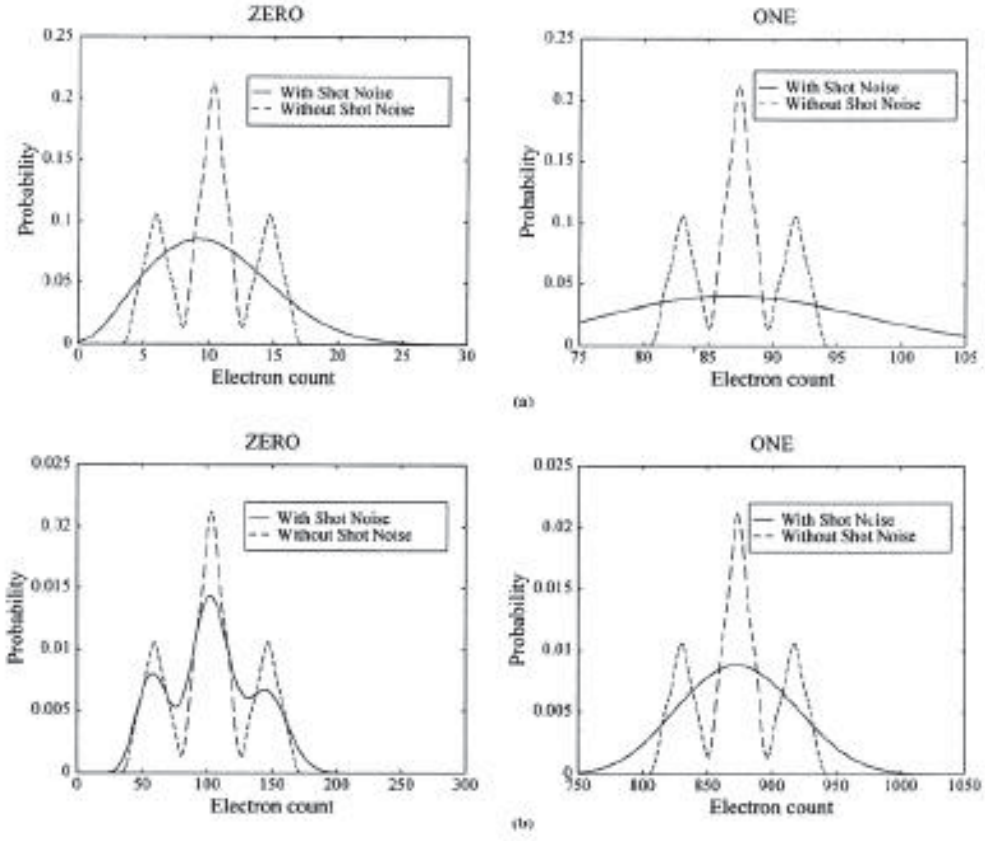

Fig. 3: probability function of the non Gausian part of the decision variable in a 40-channel WDMA system using PIN detector, (a) input optical power=-45dBm, (b) input optical power=-35dBm

An optimum threshold level β is required to calculate the error probability. This value of β minimizes the error probability and is given by (24). Optimum β as a function of signal to thermal noise ratio, using accurate method and Gaussian approximation, has been calculated and the results are presented in Fig. 4. According to Fig. 4., increase in SNR causes decrease in the optimum threshold level. This is due to the unequal decreases in variances of the decision variables related to ZERO and ONE. In fact, since shot noise, which is the dominant factor at low thermal noise powers, is signal dependent the decrease in variance of the decision variable related to ZERO is more than the decrease for ONE causing the threshold level to move to the lower values.

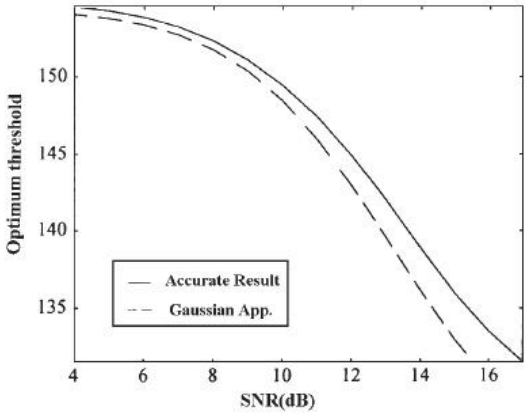

Fig. 4: Optimum threshold versus SNR

Fig. 5 is the plot of error probability versus signal to thermal noise ratio (SNR) for different optical powers in a 40-channel WDMA system with PIN photo detector and a bit rate of 2 Gb/s. Results of our calculations when shot noise is ignored are also plotted in Fig.5. It is seen that the results corresponding to the larger input powers are closer to the no-shot noise case, i.e., the degrading effect of shot noise on system performance decreases

with increase in the input power. It is also evident from Fig. 5 that when the thermal noise decreases (or SNR increases), the degrading effects of shot noise increase.

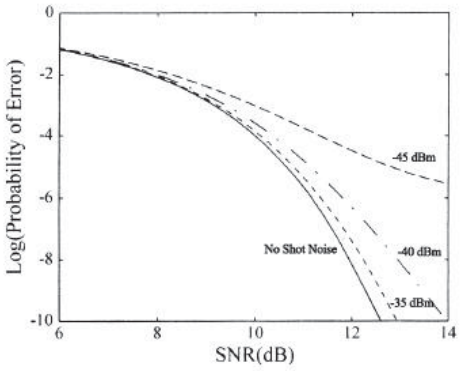

Fig. 5: Probability of error versus SNR for the system of Fig.3 for different input optical powers

The results of our calculations of error probability for a 60-channel WDMA system in presence of PIN photo detector with P_{in} = - 40 dBm and a bit rate of 2 GB/s are compared in Fig. 6. As can be seen, for small values of SNR where thermal noise is dominant, Gaussian and accurate results are very close together and as SNR increases they diverge. This is because for higher values of SNR (or lower values of thermal noise) the non-Gaussian parts (crosstalk, ISI, and shot noise) are the dominant factors. It is also apparent from Fig. 6 that among different approximations, modified Chernoff bound (MCB) is closest to the accurate results.

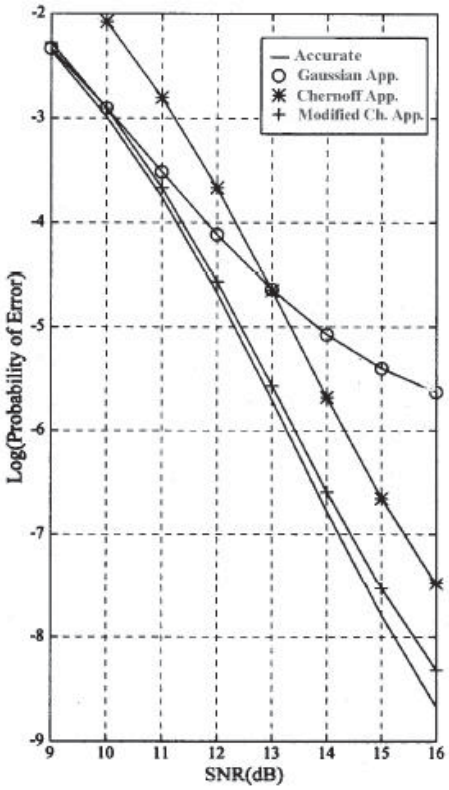

Fig. 6: Probability of error versus SNR in a 60-channel WDMA system

Results of our calculations of photo detector noise penalty and optimum gain of APD in a WDMA system with different number of channels are presented and discussed below. The photo detector noise penalty is defined as:

$$\text{Penalty} = 10\log\left(\frac{p'}{p}\right) \qquad (34)$$

where p' is the optical power required to achieve certain error probability (10^{-9} in this work) in presence of photo detector noise and p is the required optical power when photo detector noise is absent. Shot noise penalty as a function of thermal noise power in a WDMA system with PIN photo detector is presented in Fig. 7 for different number of channels. For APD receivers, the detector noise penalties are plotted in Figs. 8a and 8b for average gains of 10 and 50 respectively. In both cases the bit rate is 500 Mb/s and F=100. From Figs. 7, 8a and 8b it is apparent that the power penalty increases as the number of channels increases.

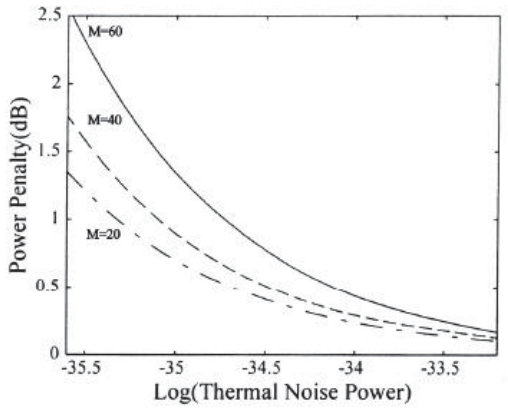

Fig. 7: Power penalty versus thermal noise in WDMA systems with different number of channels in presence of PIN photo detector

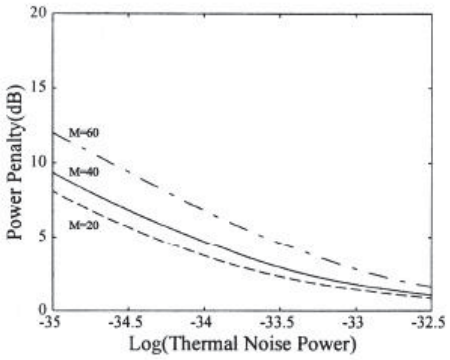

Fig. 8b: Power penalty versus thermal noise power in WDMA systems with different number of channels in presence of APD with G=50

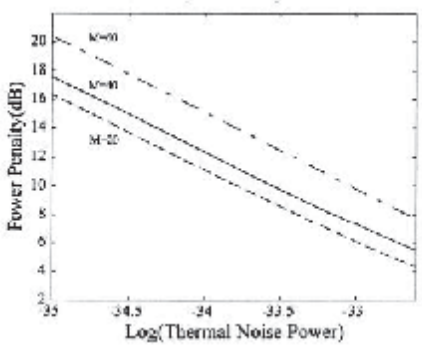

Fig. 8b: Power penalty versus thermal noise power in WDMA systems with different number of channels in presence of APD with G=50

Another important factor in system design is the optimum avalanche gain. Since the variance of the decision variable is proportional to the avalanche gain G, when the avalanche gain is increased the performance of the system is degraded. On the other hand, APD gain enlarges the signal to thermal noise ratio (SNR). Hence, there must exist an optimum gain that improves the overall system performance. However, if the receiver sensitivity is defined as the optical power required for certain probability of error (10^{-9}), then the optimum gain of APD is a value of the gain that minimizes the sensitivity. Fig. 9 shows the receiver sensitivity as a function of APD gain for different ionization rate ratios (γ) in a 40-channel WDMA system with a bit rate of 1 GB/s and an error probability equal to 10^{-9}. From Fig. 9 it is seen that an optimum gain exists resulting in the desired error probability (10^{-9}) with minimum possible input power. Also, as can be seen from Fig. 9, for small gains where the thermal noise, crosstalk, and ISI are the dominant factors, receiver sensitivity is independent of (γ) while for larger gains where the APD noise dominates, the sensitivity considerably depends on APD characteristic, that is, the smaller the ionization ratio, the smaller the excess noise factor (F), and hence, the better the system performance.

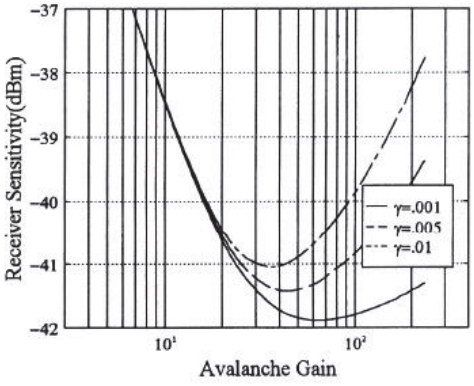

Fig. 9: Receiver sensivity versus avalanche gain in a 40-channel WDMA system with bit rate of 1 Gb/s

The optimum avalanche gain of APD and the error probability of WDMA system versus SNR for different number of channels when P_{in} = -40 dBm and the bit rate is equal to 1 Gb/s are plotted in Figs.10 and 11, respectively. It is noted that in calculations of the error probability, for each value of thermal noise power the corresponding optimum gain has been used. However, it is seen that the number of channels does not have a significant effect on the optimum gain of APD, but, as expected, the probability of error increases with increase in the number of channels.

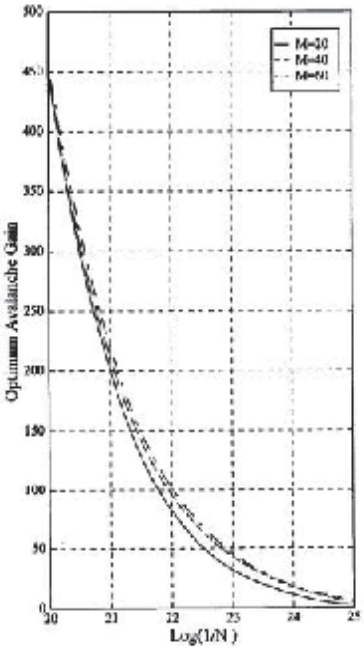

Fig-10: Optimum avalanche gain of APD versus SNR in WDMA systems with different number of channels and with a bit rate of 1 Gb/s and input power of -40dBm

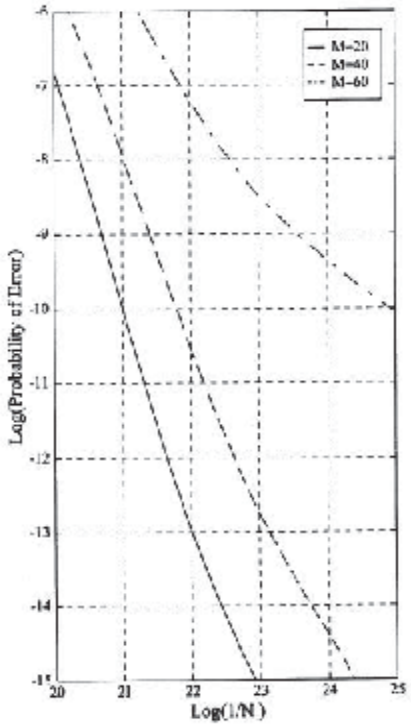

Fig. 11: Probability of error versus SNR in presence of APD for different number of channels in the system of Fig.10

The sensitivities of PIN and APD receivers versus the number of channels are plotted and compared in Figs. 12 and 13 for two different noise powers. The numbers printed on APD curves are the corresponding optimum gains. In these calculations the ionization rate ratio (γ) and the bit rate are 0.005 and 1Gb/s respectively. Also, the noise power spectral densities in Figs. 12 and 13 are 10^{-23} and 10^{-24} Amp/Hz respectively. Superiority of APD over PIN is evident from these results. However, since in WDMA systems with high number of channels the dominant factor in system performance is crosstalk, the superiority of APD over PIN decreases when the number of channels increases. Comparison of the results presented in Figs. 12 and 13 shows that as the thermal noise power increases, the advantage of APD over PIN photo detector increases. For example, as can be seen, in a 40 channels WDMA system when the noise power is equal to 10^{-24} Amp^2/Hz, the advantage of APD over PIN is 8 dB while for the higher noise power of 10^{-23} Amp^2/Hz the advantage is increased to 12 dB.

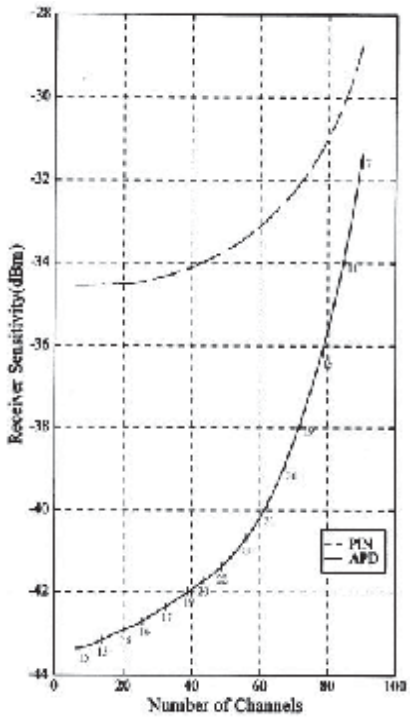

Fig. 12: Comparison of PIN and APD receiver sensivity when γ=0.005, bit rate is equal to 1 Gb/s and $N_o=10^{-24}$ Amp^2/Hz

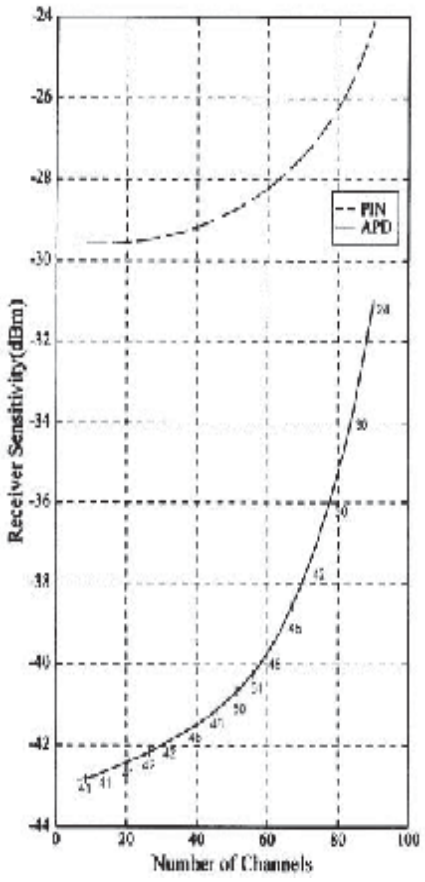

Fig. 13: Comparison of PIN and APD receiver sensivities when $N_o=10^{-23}$ Amp^2/Hz

7. Conclusion

In this paper a comprehensive analysis of the performance of WDMA systems with OOK modulation in presence of crosstalk, ISI, photo detector noise, for both APD and PIN photo detector receivers have been presented.

Probability of error with respect to signal to thermal noise ratio was calculated for different number of channels using accurate and approximate methods. It was shown that, among different approximations, the modified Chernoff bound was closest to the accurate results. The optimum gain of APD, which minimized the receiver sensitivity, was calculated for different values of ionization rate ratios and different number of channels. It was shown that the optimum gain did not change considerably with the number of channels. The photo detector power penalty was calculated as a function of thermal noise power for both APD and PIN and for different number of channels. These calculations showed that the power penalty in a WDMA system increased as the number of channels increased. The superiority of APD over PIN photo detector was demonstrated quantitatively by plotting the receiver sensitivity as a function of the number of channels for different noise powers. It was shown that the superiority of APD over PIN photo detector increased at lower number of channels and higher noise powers.

Appendix:

Calculations of the MGF of Z′:

The random variable Z′ given by eq. (3) is in fact the total number of photo electrons released from the photo detector in time interval [0,T]. The randomness of Z′ is due to two different random phenomenons: i) the randomness of the incident beam to the photo detector ii) the random nature of the photoelectron emission from the photo detector (even for a deterministic incident beam). Hence, we first calculate the conditional MGF of Z′ conditioned on the incident optical energy to the photo detector, and then average it over all possible values for the incident energies. Since the behaviors of the PIN and APD are different, each case is investigated separately as follows:

A.1. MGF of Z′ when PIN is Employed:

The total number of photo electrons emitted in time interval [0,T] from the PIN, assuming $\rho=0$ for simplicity, is a Poisson process given by:

$$Z' = \frac{1}{e}\int_0^T i(t)dt = \sum_n h_e(T - t_n) \qquad (a.1)$$

Where, t_ns are the random Poisson points, $h_e(t) = h_d(t) * h_r(t)$, $h_d(t)$ and $h_r(t)$ are the impulse responses of the photo detector and I&D filter respectively, and * is the convolution signe.

For this process, the Poisson parameter q , defined as the average number of photo electrons emitted in unit time from the PIN, is equal to the total incident energy in time interval [0,T] to the PIN. From the definition of $\lambda(t)$ in eq.(7) and from eq.(6), we can write:

$$q = \int_0^T \lambda(t)dt = X \qquad (a.2)$$

For the ideal cases, where $h_d(t) = e\delta(t)$ and $h_r(t) = U(t)/e$, eq.(a.1) becomes:

$$Z' = \sum_n U(T - t_n) \qquad (a.3)$$

The conditional MGF of Z′ conditioned on X is straightforward and has been derived by [16] as:

$$\Phi_{z'|x}(s) = E\left\{e^{sZ'}\middle|X\right\} = \exp\left[(e^{s}-1)X\right] \qquad \text{(a.4)}$$

From this, the MGF of z' is obtained by averaging $\Phi_{z'|x}(s)$ over all possible X's, hence:

$$\Phi_{z'}(s) = E_x\left\{\Phi_{z'|x}(s)\right\} = E_x\left\{\exp\left[(e^{s}-1)X\right]\right\} \quad \text{(a.5)}$$

By the definition of MGF we have:

$$\Phi_{x}(s) = E\left\{\exp(sX)\right\} \qquad \text{(a.6)}$$

Comparing eq.(a.5) with eq.(a.6) , we can write the MGF o f Z′ with respect to the MGF of X as :

$$\Phi_{z'}(s) = \Phi_{x}(e^{s}-1) \qquad \text{(a.7)}$$

A.2. MGF of Z′ when APD is Employed:

The MGF of Z′ conditioned on the incident optical energy X has been investigated by [18] and is given by:

$$\Phi_{z'|x}(s) = \exp\left[\int_0^T \left\{\Phi_G\left[\mathrm{Sh}_e(T-\alpha)\right]-1\right\}\lambda(\alpha)d\alpha\right] \qquad \text{(a.8)}$$

where, $\Phi_G(s)$ is the MGF of the random gain G of APD given in eq. (9).

For the ideal situations, similar to the PIN case, eq. (a.8) becomes:

$$\Phi_{z'|x}(s) = \exp\left\{\left[\Phi_G(s)-1\right]\int_0^T \lambda(\alpha)d\alpha\right\} \qquad \text{(a.9)}$$

Using eq. (6), the above equation can be written as:

$$\Phi_{z'|x}(s) = \exp\left\{\left[\Phi_G(s)-1\right]X\right\} \qquad \text{(a.10)}$$

From this equation, similar to eq.(a.5) , we can write:

$$\Phi_{z'}(s) = E_x\left\{\exp\left\{\left[\Phi_G(s)-1\right]X\right\}\right\} \qquad \text{(a.11)}$$

Comparing this with eq. (a.6), results in the following equation for the MGF of Z′ with respect to the MGF of X :

$$\Phi_{z'}(s) = \Phi_x\left[\Phi_G(s)-1\right] \qquad \text{(a.12)}$$

So far we have calculated the MGF of the random variable Z′ in terms of the MGF of the random variable X for both APD and PIN photo detectors.

To complete the task, the MGF of X is required which has been found in the paper from the statistical properties of the data and noise etc.

References

[1] I. P. Kaminow, P. Iannone, J. Stone, and J. W. Stulz, "FDMA-FSK" star network with a tunable optical filter demultplexer", J. of Lightwave Technol., vol. 6, pp. 1406-1414, 1988.

[2] M. S. Goodman, "Multiwavelength network and new approaches to packet switching", IEEE Commum. Mag., vol. 27, no. 10, pp. 27, Oct. 1989.

[3] Y. M. Lin, D.R. Spears and M. Yin. "Fiber-based local access network architectures", IEEE Commun. Mag., vol. 27, no. 10, pp. 64, Oct. 1989.

[4] B. Mukherjee, "WDM optical communication network: progress and challenges", IEEE J. of selected Areas in Communications, vol. 18, no. 10, October 2000.

[5] C. Fan, "Keynotes address–optical networking: A paradigm shift", in WDM Forum, London, June 1998.

[6] [6] J. Nagel, "Prospects for optical networking", in (D) WDM Forum, Phoenix, AZ, Oct. 1998.

[7] M. Moulavi-Kakhki and M. Kavehrad, " Holographic optical filters and cross-talk performance in WDM networks", J. of Optical Communications, Vol. 16, pp.190-193, 1995

[8] Ioannis E Pountourakis, " Asynchronous transmission WDM networks with performance efficiency improvement", IEEE Communication Letters, Vol.7, No. 8, Aug. 2003.

[9] Stock and Edward H. Sargent, "System performance comparison of optical CDMA and WDMA in a broadcast local –area network", IEEE Communication Letters, Vol.6, No. 9, pp 409-411, Sept. 2002

[10] C. S. Li et al., "Channel capacity optimization of chirp limited dense WDM/WDMA system using OOK/FSK modulation and optical filters", J. of Lightwave Technol., vol. 10. pp. 1148-1161, 1992.

[11] L. J. Cimini and G. J. Foschini. " Can multilevel signaling improve the spectral efficiency of ASK optical FDM system", IEEE Trans. On Commun., vol. 41, pp. 1048-1090, 1993.

[12] A. M. Hill and D. B. Payne, " Linear crosstalk in wavelength division multiplexed optical fiber transmissions system", J. of Lightwave Technol., vol. 3, pp.643-651, 1985.
[13] P. A. Rosher and A. R. Hunwicks. "The analysis of crosstalk in multi channel wavelength division multiplexer", IEEE J. of selected Areas in Commun., vol. 9, pp. 1108-1115, 1990.
[14] S.Geekler, "Crosstalk penalties in a bidirectional fiber optic WDM system", IEEE J. of Selected Areas in Commun., vol. 9, pp. 1115-1120 1990.
[15] W. H. Hamdy and P. A. Humblet, "Sensitivity analysis of direct detection optical FDMA network with OOK modulation", J. of Lightwave Technol., vol. 11, pp. 783-794, 1993.
[16] A. Papoulis," Probabitiy, Random Variables, and Stochastic Processes", 3rd ed. McGraw-Hill, 1991.
[17] D. L. Snyder," Random Point Processes", New York : Wiely, 1975.
[18] S. D. Personick, "Statistics of a general class of avalanche detectors with application to optical communication", Bell system Techn. J., vol. 50, pp.3075-3095, Dec. 1971.
[19] K. E. House, "Detection and equalization in fiber-optical communication", Ph.D dissertation, Univ. Essex, England, 1979.
[20] J. G. Prokis, Digital Communications. 3nd ed., McGraw-Hill, 2001.
[21] J. J. O Reilly and J. R. F. da Rocha, "Improved error probability evaluation methods for direct detection optical communication systems", IEEE Trans. On Information Theory, vol. IT-33, pp 839-848, Nov. 1987.